

# Mobile robot SLAM for line-based environment representation

Andrea Garulli, Antonio Giannitrapani, Andrea Rossi, Antonio Vicino

Dipartimento di Ingegneria dell'Informazione

Università di Siena

Via Roma 56, 53100 Siena, Italy

{garulli, giannitrapani, rossiandr, vicino}@dii.unisi.it

**Abstract**—This paper presents an algorithm for solving the simultaneous localization and map building (SLAM) problem, a key issue for autonomous navigation in unknown environments. The considered scenario is that of a mobile robot using range scans, provided by a 2D laser rangefinder, to update a map of the environment and simultaneously estimate its position and orientation within the map. The environment representation is based on linear features whose parameters are extracted from range scans, while the corresponding covariance matrices are computed from the statistical properties of the raw data. Simultaneous update of robot pose and linear feature estimates is performed via extended Kalman filtering. Experimental tests performed within a real-world indoor environment demonstrate the effectiveness of the proposed SLAM technique.

## I. INTRODUCTION

Simultaneous localization and map building (SLAM) is a challenging problem in mobile robotics that has attracted the interest of more and more researchers in the last decade. Self-localization of mobile robots is obviously a fundamental issue in autonomous navigation: a mobile robot must be able to estimate its position and orientation (pose) within a map of the environment it is navigating in. However, in many applications of practical relevance (like exploration tasks or operations in hostile environments), a map is not available or it is highly uncertain. Therefore, in such cases the robot must use the measurements provided by its sensory equipment to estimate a map of the environment and, *at the same time*, to localize itself within the map.

Several techniques have been proposed so far to tackle the SLAM problem. The main difference between them concerns basically the environment representation and the uncertainty description (see [1] for a comprehensive review of map building techniques). A wide variety of localization and mapping techniques relies on environment representations consisting of a set of characteristic elements detectable by the robot sensory system (*feature-based* maps). A typical scenario is that of a robot measuring its relative range and/or bearing with respect to pointwise landmarks. In this setting, localization algorithms with known landmarks and SLAM techniques have been devised both for a statistical description of the sensor uncertainty (e.g. [2], [3]) and in a bounded-error framework (e.g. [4], [5], [6]).

Lines and segments are another class of commonly used features [7]. They are especially suited for indoor applications as they can be effectively extracted from range scans and then exploited for localization and/or mapping

purposes. An algorithm for computing the relative displacement between two different robot poses by aligning the corresponding range scans has been presented in [8]. In this context, fitting lines are instrumental to the solution of the point-to-point correspondence problem. A method for building a line-based map, accounting for both robot pose and measurement uncertainty, can be found in [9]. An alternative mapping technique has been proposed in [10]. It is based on an improved line extraction scheme, which explicitly takes into account each point uncertainty in the computation of the line parameters. However, both [9] and [10] do not explicitly address the SLAM problem. Recently, a segment-based SLAM algorithm exploiting 3D laser scans has been proposed in [11]. It builds a 2D map of the environment, which is at same time used for localizing the robot, by projecting on the horizontal plane readings of a 3D laser range finder.

In this paper we present a SLAM algorithm based on range scans delivered by a 2D laser rangefinder and adopting a line-based description of the environment. The problem is cast as a state estimation problem for an uncertain dynamic system, whose state vector includes both the robot pose and the line parameters in a global reference frame. The covariance matrices associated to the parameters of the linear features are explicitly computed from those of the raw data delivered by the sensors, and then fed into an Extended Kalman Filter (EKF) which simultaneously estimates the current robot pose and updates the map. In order to facilitate data association, the EKF is enhanced by keeping track of segments associated to line features.

The paper is organized as follows. The SLAM problem is formulated in Section II. The EKF-based algorithm is briefly reviewed in Section III. Section IV describes the line extraction technique, as well as the computation of the covariance matrix of the line parameters from those of the raw data. Feature matching and map management are discussed in Section V. Results of experimental tests performed in a real-world indoor environment are reported in Section VI, while conclusions and future lines of research are outlined in Section VII.

## II. PROBLEM FORMULATION

Let us consider an autonomous vehicle navigating in a 2D environment and let  $p(k) = [x(k), y(k), \theta(k)]'$  denote its pose (i.e., the position  $x(k), y(k)$  and orientation  $\theta(k)$ )

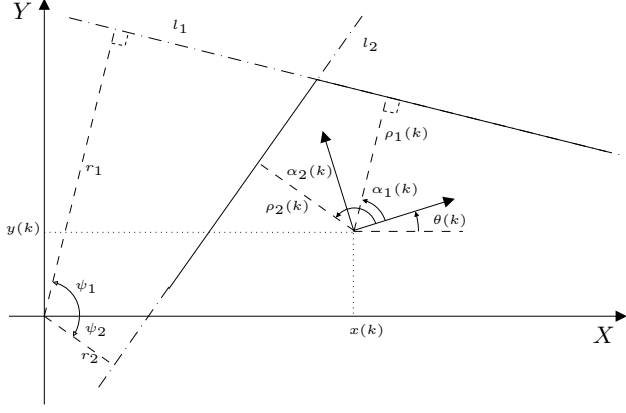


Fig. 1. Line parameters  $[r, \psi]'$  are expressed w.r.t. the global reference frame. Line parameters  $[\rho, \alpha]'$  are expressed w.r.t a robot-centered reference frames.  $[x, y, \theta]'$  denote the robot pose w.r.t. the global reference frame.

at time  $k$ , in a global reference frame. The environment is described by static rectilinear features (like portions of walls, doors, shelves) detectable by the robot sensory system. In this scenario, a suitable environment representation can be given in terms of the lines underlying each feature. A line  $l_i = [r_i, \psi_i]'$  is parametrized by its distance  $r_i \geq 0$  from the origin and the direction  $\psi_i \in (-\pi, \pi]$  of the normal passing through the origin (see Figure 1). Given a robot kinematic model and a measurement equation, the simultaneous localization and map building problem can be cast as a state estimation problem for an uncertain dynamic system. To illustrate the main ideas, let us suppose that the agent pose evolves according to the simple linear model

$$p(k+1) = p(k) + u(k) + w(k), \quad k = 0, 1, \dots \quad (1)$$

where  $w(k) \in \mathbb{R}^3$  models the noise affecting the odometric measurements  $u(k) \in \mathbb{R}^3$ . Nonetheless, more general kinematic models of the form  $p(k+1) = \varphi(p(k), u(k), w(k))$  can be dealt with in the proposed framework.

Assume that at each time instant  $k$ , the robot is able to measure the distance  $\rho_i(k)$  and orientation  $\alpha_i(k)$  of the  $i$ -th feature from its current pose  $p(k)$  (see Figure 1). Let  $z_i(k) = [\rho_i(k), \alpha_i(k)]'$ ,  $i = 1, \dots, n$  denote the parameter measurements of the  $i$ -th feature in a robot centered reference frame. Then,  $z_i(k)$  can be expressed as a function  $\mu_i(p(k), l_i)$  of the current vehicle pose  $p(k)$  and the parameters  $l_i$  of the sensed feature in the global reference frame:

$$z_i(k) = \mu_i(p(k), l_i) + v_i(k), \quad (2)$$

where  $v_i(k) \in \mathbb{R}^2$  models the noise affecting the  $i$ -th measurement. Depending on whether the segment joining the vehicle position  $x(k), y(k)$  and the origin intersects or not the line  $l_i$ , the measurement equation takes on the form:

$$\mu_i(p(k), l_i) = \begin{bmatrix} -r_i + x(k) \cos(\psi_i) + y(k) \sin(\psi_i) \\ \psi_i - \theta(k) + \pi \end{bmatrix} \quad (3)$$

or

$$\mu_i(p(k), l_i) = \begin{bmatrix} r_i - x(k) \cos(\psi_i) - y(k) \sin(\psi_i) \\ \psi_i - \theta(k) \end{bmatrix}. \quad (4)$$

Let us rearrange all the quantities to be estimated (i.e. the robot pose  $p(k)$  and the line parameters  $l_i$ ) into a state vector  $\xi(k) \in \mathbb{R}^{3+2n}$ :  $\xi(k) = [p(k)', l_1', \dots, l_n']'$ . Since static feature are considered, from (1) the time evolution of the state vector is given by:

$$\xi(k+1) = \xi(k) + E_3 u(k) + E_3 w(k) \quad (5)$$

where  $E_3 = [I_3 \ 0_{3 \times 2n}]' \in \mathbb{R}^{(3+2n) \times 3}$ . Finally, if the measurements taken at time  $k$  are stacked into a vector  $z(k) = [z_1(k)', \dots, z_n(k)']' \in \mathbb{R}^{2n}$ , the measurement equation (2) can be rewritten as:

$$z(k) = \mu(\xi(k)) + v(k) \quad (6)$$

where  $\mu(\xi(k)) = [\mu_1(p(k), l_1)', \dots, \mu_n(p(k), l_n)']'$  and  $v(k) = [v_1(k)', \dots, v_n(k)']'$ . Now, the SLAM problem can be stated as follows.

**SLAM problem.** Let  $\hat{\xi}(0)$  be an estimate of the initial robot position and feature parameters. Given the dynamic model (5) and the measurement equation (6), find an estimate  $\hat{\xi}(k)$  of the robot pose and feature parameters  $\xi(k)$ , for each  $k = 1, 2, \dots$ .

### III. EXTENDED KALMAN FILTERING

The main advantage of the above formulation is that any state estimation technique can be used to address the SLAM problem. When a statistical description of the uncertainty is adopted, the standard approach is that based on the Extended Kalman Filter (EKF). Let the process disturbance  $w(k)$  and the measurement noise  $v(k)$  be modelled as zero-mean, white noise, with covariance matrices  $Q(k) \in \mathbb{R}^{3 \times 3}$  and  $R(k) \in \mathbb{R}^{2n \times 2n}$ , respectively. Let  $\hat{\xi}(k|k)$  denote the state estimate at time  $k$ , based on all the measurements collected up to that time, and let  $P(k|k)$  be the covariance matrix of the corresponding estimation error. The estimate update is carried out in two stages as summarized below.

*Prediction:*

$$\begin{aligned} \hat{\xi}(k+1|k) &= \hat{\xi}(k|k) + E_3 u(k) \\ P(k+1|k) &= P(k|k) + E_3 Q(k) E_3' \end{aligned}$$

*Correction:*

$$\begin{aligned} \hat{\xi}(k+1|k+1) &= \hat{\xi}(k+1|k) + \\ &\quad + K(k+1)(z(k+1) - h(\hat{\xi}(k+1|k))) \\ P(k+1|k+1) &= P(k+1|k) + \\ &\quad - K(k+1)S(k+1)K(k+1)' \\ K(k+1) &= P(k+1|k)H(k+1)'S(k+1)^{-1} \\ S(k+1) &= H(k+1)P(k+1|k)H(k+1)' + R(k+1) \end{aligned}$$

where  $H(k+1) = \left. \frac{\partial \mu(\xi)}{\partial \xi} \right|_{\xi = \hat{\xi}(k+1|k)}$ .

### IV. FEATURE EXTRACTION

The EKF recursion is based on the measurements  $z(k)$ , which are not directly available to the robot but must be extracted from the readings provided by the robot sensory equipment. The extraction of lines from range scans is a widely studied problem and several solutions are available

(see e.g., [9], [10] and reference therein). The approach adopted in this paper to obtain the measurements  $z(k)$ , as well as the corresponding covariance matrix  $R(k)$ , is described in the following. The robot is supposed to be equipped with a proximity sensor (e.g., sonar rings or laser rangefinder) providing  $N$  range and bearing measurements:  $[d_j, \phi_j]'$ ,  $j = 1, \dots, N$ , where  $d_j$  is the distance of the point sensed along the direction  $\phi_j$ . The sensor readings are processed in order to extract the parameters  $[\rho_h(k), \alpha_h(k)]'$  of the linear features present in the surroundings, by iteratively alternating *segmentation* and *line fitting* steps. The segmentation phase aims at identifying the sensor readings belonging to the same feature, while the line fitting algorithm allows to compute the feature parameters given a set of related points. In the following, for notational clarity the time dependence will be omitted.

The pair  $[d_j, \phi_j]'$  can be thought of as the polar coordinates of the  $j$ -th point in a robot centered reference frame. Let us denote by

$$p_j = [x_j, y_j]' = [d_j \cos(\phi_j), d_j \sin(\phi_j)]', \quad (7)$$

the Cartesian coordinates of the  $j$ -th point referenced to the same frame. The segmentation phase consists in partitioning the sensor readings into subsets  $S_h$  (called *segments*) of “almost collinear” points:  $S_h = \{p_1^{(h)}, \dots, p_{n_h}^{(h)}\}$ ,  $h = 1, \dots, q$ , where  $n_h$  denotes the cardinality of the  $h$ -th segment. Each set is built iteratively. All the points  $p_j$  are processed sequentially, with the first two initializing the segment  $S_1$ . Then, a point  $p_j$ , is added to the current segment if it satisfies the following criterion:

- its normal distance from the current fitting line is below a threshold  $\delta_0$ , and
- its Euclidean distance from the last point in the current segment is below a threshold  $\delta_1$ .

When a new point is inserted in the current segment, the parameters of the fitting line are recomputed on the basis of the new set of points. If  $N_p$  consecutive points do not meet the above criterion, the current segment  $S_h$  is assumed to be completed, and a new one  $S_{h+1}$  is instantiated, starting from the next point with respect to the last one inserted into  $S_h$ . Notice that, the condition which determines the end of a segment allows to filter out spurious readings (outliers) due to small projections, indentations or occlusions of a flat surface. Moreover, in order to increase the robustness of the extraction phase and reject false features, segments shorter<sup>1</sup> than a minimum length  $L_0$  or made up of less than  $N_0$  points are deemed unreliable and are discarded.

Once a segment  $S_h$  has been identified, the parameters of the corresponding linear feature  $[\rho_h, \alpha_h]'$  are computed by fitting a line through all the points belonging to  $S_h$ . Let  $p_i^{(h)} = [x_i^{(h)}, y_i^{(h)}]'$ , be the coordinates of the  $i$ -th point in  $S_h$ ,  $i = 1, \dots, n_h$ . The normal distance of  $p_i^{(h)}$  to the line  $l$  described by the parameters  $[\rho, \alpha]'$  is given by  $d(p_i^{(h)}, l) =$

<sup>1</sup>The length of a segment  $S_h$  has to be intended as the distance between the first  $p_1^{(h)}$  and last  $p_{n_h}^{(h)}$  points in  $S_h$ .

$|\rho - x_i^{(h)} \cos(\alpha) - y_i^{(h)} \sin(\alpha)|$ . Then, the parameters of the fitting line are computed by minimizing the cost function

$$[\rho_h, \alpha_h]' = \arg \min_{\rho, \alpha} E(\rho, \alpha), \quad h = 1, \dots, q \quad (8)$$

where  $E(\rho, \alpha) = \sum_{i=1}^{n_h} (\rho - x_i^{(h)} \cos(\alpha) - y_i^{(h)} \sin(\alpha))^2$ . The solution of the optimization problem (8) can be analytically computed as a function of the points  $p_i^{(h)}$  concurring to define the current line. Recalling equation (7), the parameters of the  $h$ -th feature can be written as a function  $s: \mathbb{R}^{2n_h} \rightarrow \mathbb{R}^2$  of the sensor readings (see the Appendix):

$$[\rho_h, \alpha_h]' = s(d_1^{(h)}, \phi_1^{(h)}, \dots, d_{n_h}^{(h)}, \phi_{n_h}^{(h)}). \quad (9)$$

The line parameters extracted according to the above procedure represent the measurements (6) used to update the state estimate. However, in the EKF correction step the knowledge of the covariance matrix  $R(k)$  of the observation noise  $v(k)$  is also required. This information can be approximated, through linearization of equation (9), from the statistical properties of the errors affecting the raw data delivered by the sensor. Let

$$C_{m_i} = \begin{bmatrix} \sigma_{d_i}^2 & \sigma_{d_i \phi_i} \\ \sigma_{\phi_i d_i} & \sigma_{\phi_i}^2 \end{bmatrix}$$

be the covariance matrix of the noise affecting the sensor reading  $[d_i^{(h)}, \phi_i^{(h)}]'$ . Assuming that the errors corrupting different readings are uncorrelated, the covariance matrix of the  $h$ -th measurement  $z_h(k)$  can be approximated as:

$$R_h(k) = \sum_{i=1}^{n_h} J_i C_{m_i} J_i' \quad (10)$$

where the matrix  $J_i \in \mathbb{R}^{2 \times 2}$  is the Jacobian of  $s(\cdot)$  w.r.t. the pair  $d_i^{(h)}, \phi_i^{(h)}$  (full expressions are reported in the Appendix). Finally, because of the hypothesis of uncorrelated measurement noise, the covariance matrix  $R(k)$  has a block diagonal structure, the  $h$ -th block being  $R_h(k)$  in equation (10).

## V. MATCHING AND MAP MANAGEMENT

In order to perform the EKF correction step, each measurement  $z_h(k)$  extracted from the sensor data must be associated to the corresponding line present in the map (matching problem). This is a challenging task whenever natural features are used and the sensory system returns only metric information (like any proximity sensor), so that elements constituting the map turn out to be indistinguishable. In the following, we briefly describe the matching strategy adopted in this work.

Let

$$\hat{\xi}(k|k-1) = [\hat{p}(k|k-1)', \hat{l}_1(k|k-1)', \dots, \hat{l}_n(k|k-1)']'$$

be the state estimate at time  $k$ , before the measurements are processed. Given the current state estimate  $\hat{\xi}(k|k-1)$  and the observations  $z_h(k)$ , the matching problem consists in determining the feature  $l_i$  (if it exists) in the map, originating the  $h$ -th measurement,  $h = 1, \dots, q$ . Intuitively, one would compare the  $h$ -th extracted feature to the current line

estimates and select the “closest” one. Several heuristics can be devised to this purpose, involving different comparison criteria. In this respect, key issues that must be considered are:

- i) the comparison requires to express the extracted line parameters w.r.t. the global reference frame;
- ii) the uncertainty affecting the parameters involved in the comparison must be taken into account;
- iii) different features in the environment may lie on the same line (e.g., two aligned walls separated by a hallway).

The first issue is addressed by solving  $z_h(k) = \mu_h(\hat{p}(k|k-1), l_h)$  with respect to  $l_h$ , where  $\mu_h(\cdot, \cdot)$  is defined in (3)-(4). At the same time, the covariance  $R_h(k)$  of the extracted parameters is propagated, through linearization, according to the covariance matrix of the current robot pose estimate. To face the last problem, for each line  $\hat{l}_i(k|k-1)$  in the map, the endpoints of an associated segment are computed and updated together with the EKF recursion, in order to trace the length and the position of the physical feature along the corresponding line. It is worth remarking that the segment endpoints are not included in the state vector, but are used as an instrumental tool to enhance the matching stage.

The matching algorithm proceeds through two stages. First, for each measurement  $z_h(k)$  all possible associations are determined by using three validation gates. The parameters involved in this test are:

- a) the squared difference of orientation, weighted by the inverse of its variance, between the extracted line and the feature estimates  $\hat{l}_i(k|k-1)$ ;
- b) the squared normal distance, weighted by the inverse of its variance, of the midpoint of the extracted segment to the feature estimate  $\hat{l}_i(k|k-1)$ ;
- c) the overlapping rate between the extracted segment and the one associated to the feature estimate  $\hat{l}_i(k|k-1)$ .

Then, among all feasible correspondences, the one minimizing a cost function, typically a weighted sum involving the quantities previously computed in a)-c), is selected. When a measurement  $z_h(k)$  is associated to a feature  $\hat{l}_i(k|k-1)$ , the endpoints of the  $i$ -th segment are suitably updated, by projecting the endpoints of the extracted segment onto the corresponding line  $\hat{l}_i(k|k-1)$ .

If a measurement  $z_h(k)$  does not match any of the lines currently present in the state vector, it has to be considered as a new feature and the state vector must be properly augmented. Let us denote by  $\hat{\xi}_n(k|k) \in \mathbb{R}^{3+2n}$  the state estimate after the measurement update at time  $k$  and let  $P_n(k|k)$  be the corresponding estimation error covariance. Then, the new state vector becomes  $\hat{\xi}_{n+1}(k|k) \triangleq [\hat{\xi}_n(k|k)', \hat{l}_{n+1}(k|k)']'$  where

$$\hat{l}_{n+1}(k|k)' = [\hat{r}_{n+1}(k|k), \hat{\psi}_{n+1}(k|k)]' = \gamma(\hat{p}(k|k), z_h(k)).$$

The function  $\gamma(\hat{p}(k|k), z_h(k))$  represents the initial estimate of the newly added line (in the global reference frame) according to the current robot pose estimate and takes on

the form (see equations (3)-(4)):

$$\begin{bmatrix} \hat{r}_{n+1} \\ \hat{\psi}_{n+1} \end{bmatrix} = \begin{bmatrix} -\rho_h(k) + \hat{x}(k|k) \cos(\alpha_h(k) + \hat{\theta}(k|k) - \pi) + \\ \hat{y}(k|k) \sin(\alpha_h(k) + \hat{\theta}(k|k) - \pi) \\ \alpha_h(k) + \hat{\theta}(k|k) - \pi \end{bmatrix}$$

or

$$\begin{bmatrix} \hat{r}_{n+1} \\ \hat{\psi}_{n+1} \end{bmatrix} = \begin{bmatrix} \rho_h(k) + \hat{x}(k|k) \cos(\alpha_h(k) - \hat{\theta}(k|k)) + \\ \hat{y}(k|k) \sin(\alpha_h(k) - \hat{\theta}(k|k)) \\ \alpha_h(k) - \hat{\theta}(k|k) \end{bmatrix}$$

depending on the relative position of the vehicle and the  $(n+1)$ -th line w.r.t. the origin. Analogously, the covariance matrix  $P_n(k|k)$  becomes:

$$P_{n+1}(k|k) = \begin{bmatrix} P_n(k|k) & P_n(k|k)J'_\xi \\ J_\xi P_n(k|k) & J_\xi P_n(k|k)J'_\xi + J_z P_n(k|k)J'_z \end{bmatrix}$$

where  $J_\xi$  and  $J_z$  are the Jacobian matrices:

$$J_\xi = \frac{\partial \gamma(\hat{p}(k|k), z_h(k))}{\partial \hat{\xi}_n}, \quad J_z = \frac{\partial \gamma(\hat{p}(k|k), z_h(k))}{\partial z_h}.$$

*Remark 1:* In order to avoid the introduction of spurious features in the state vector, an unmatched measurement can be first inserted into a list of tentative features and then added to the state only when it is deemed sufficiently reliable (e.g., if it is detected at least a prescribed number of times over a given length of time [3]).

Despite the cautions taken in the extraction and matching phases, it may still happen that two initially distinct features turn out to be related to the same environment item<sup>2</sup> (e.g., a long wall with temporary occlusions, or duplication of the same feature due to a poor estimation of the current robot pose). A possible way to deal with this problem is to periodically inspect the state vector and check whether any pair of features pass the aforementioned validation gates. If that is the case, the two state components can be actually considered as two estimates of the same feature, and they can be consequently merged according to their current uncertainties.

## VI. EXPERIMENTAL RESULTS

The proposed SLAM algorithm has been validated on real data gathered during several experiments performed by a mobile robot Pioneer 3AT. This vehicle has a differential drive guide and is equipped with a SICK LMS laser rangefinder, providing 180° planar scans of the environment, with a 0.5° resolution. The results of a typical run are shown in Figure 2. The robot explores an environment constituted by four rooms of the Siena Robotics and Systems (SIRS) lab at our department, labelled from (A) to (D) in Figure 2, according to the sequence (A)-(D)-(A)-(B)-(C)-(B)-(A). The total distance travelled by the vehicle is about 170 m, at an average speed of 0.4 m/s. Along the path, the robot collects range scans at a frequency of 4 Hz and accordingly updates its pose estimate and the line-based map.

<sup>2</sup>Recall that although a physical linear feature  $l_i$  is supposed to be static, its estimates  $\hat{l}_i(k|k)$  vary during time.

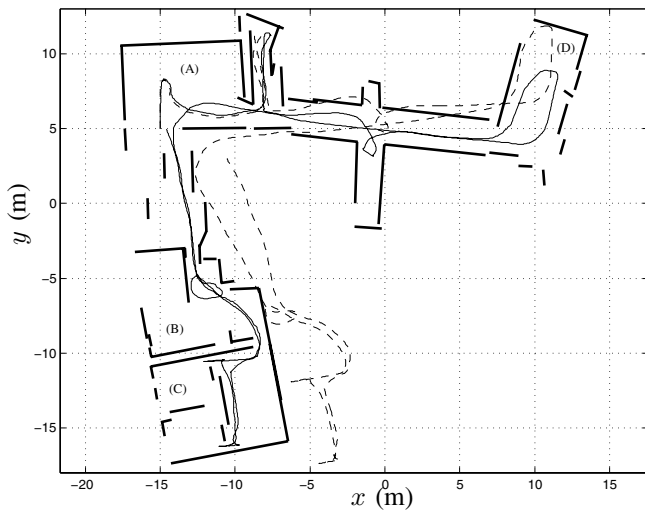


Fig. 2. Estimated trajectory by the SLAM algorithm (solid line) and by odometry (dashed); segments associated to final map (thick solid lines)

In Figure 2, the trajectory estimated by the SLAM algorithm (solid line) and the one reconstructed from encoder readings (dashed line) are depicted, together with the segments associated to the final line estimates in the map (thick solid lines). It can be noticed the poor quality of odometric estimates which after the first turns rapidly begin to drift away from the actual vehicle position; the error accumulated at the end of the run is about  $4.5\text{ m}$ . The effectiveness of the SLAM algorithm to compensate for odometric errors is clear from the final position and orientation errors, smaller than  $0.07\text{ m}$  and  $0.5^\circ$ , respectively. Although the ground truth is available only for the initial and final positions, nonetheless satisfactory estimation accuracy along the path can be observed, by looking at Figures 3-4 where 70 range scans taken during the experiment are plotted according to the current odometric estimate (Figure 3) or to the current SLAM algorithm estimate (Figure 4).

The final map built by the SLAM technique is composed of 66 features. The parameters of the segmentation procedure have been tuned trading-off the accuracy of the extracted lines and the need to account for several unevennesses characterizing real-world features. The overall map management based on a tentative list and line merging, resulted in the rejection of 48 spurious lines and the fusion of 19 map elements. It is worth noticing that the misalignment among the rooms actually resembles the shape of the building (dating back to the 15th century) and is not due to mapping faults. The presence of slightly curved walls or occlusions caused an over-segmentation of the map which in some cases, as a result of a wrong matching, generated overlapping segments corresponding to nominally different features. However, despite these drawbacks, the map accuracy proved to be very well suited for navigation purposes, allowing the robot to traverse back and forth different rooms without getting lost.

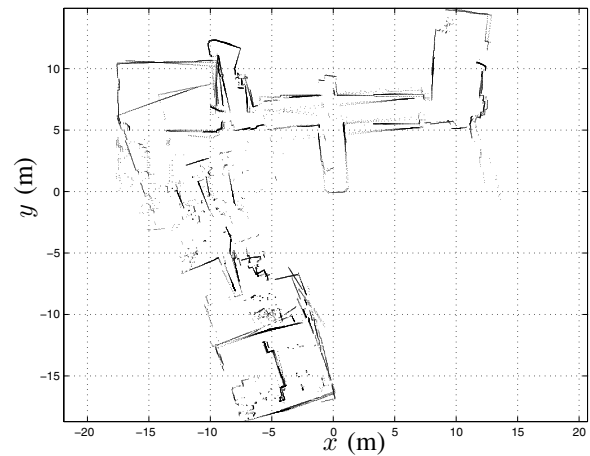


Fig. 3. Raw data relative to odometric pose estimates.

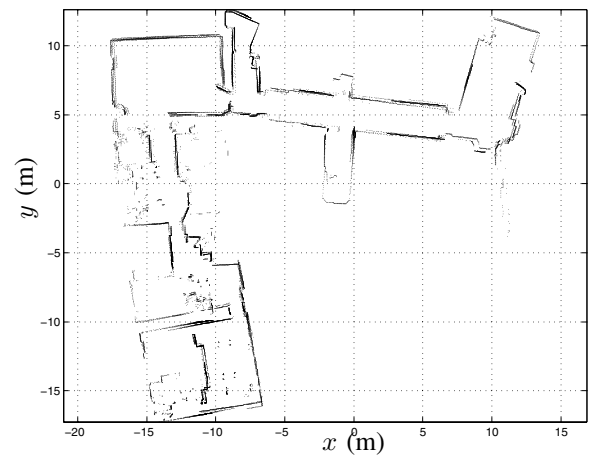


Fig. 4. Raw data relative to SLAM algorithm pose estimates.

## VII. CONCLUSION AND FUTURE WORK

In this paper, a simultaneous localization and mapping technique for mobile robots navigating in indoor environments has been presented. By adopting a line-based representation of the environment, the problem is cast as a state estimation problem and solved via extended Kalman filtering. The results of experimental validation, carried out using the mobile platform Pioneer 3AT, confirm the viability of the proposed approach in quite complex indoor environments.

Future directions of research include the integration of additional features in the map (e.g. corners or pointwise landmarks) and the comparison with different segmentation algorithms (e.g., [10]) as well as with more sophisticated data association policies (e.g., [12]). The ability of the proposed SLAM technique to deal with large loops is a current subject of study. In this respect, preliminary promising results have been obtained by simulation experiments. Moreover, the consistency of the line-based map in the long run (see [13]) is under investigation.

## APPENDIX

Let us consider  $n$  points  $p_i = [x_i, y_i]'$ ,  $i = 1, \dots, n$  on a plane. The line  $l = [\rho^*, \alpha^*]'$  minimizing the sum of the squared normal distances from each point  $E(\alpha, \rho) = \sum_{i=1}^n (\rho - x_i \cos(\alpha) - y_i \sin(\alpha))^2$  is given by the function  $f = [f_1, f_2]'$ :

$$\begin{bmatrix} \rho^* \\ \alpha^* \end{bmatrix} = \begin{bmatrix} \bar{x} \cos(\alpha^*) + \bar{y} \sin(\alpha^*) \\ \frac{1}{2} \arctan \frac{-2S_{xy}}{S_{y^2} - S_{x^2}} \end{bmatrix} \triangleq \begin{bmatrix} f_1(x_1, y_1, \dots, x_n, y_n) \\ f_2(x_1, y_1, \dots, x_n, y_n) \end{bmatrix} \quad (11)$$

where (see [8]):

$$\begin{aligned} \bar{x} &= \frac{1}{n} \sum_{i=1}^n x_i, & \bar{y} &= \frac{1}{n} \sum_{i=1}^n y_i, \\ S_{x^2} &= \sum_{i=1}^n (x_i - \bar{x})^2, & S_{y^2} &= \sum_{i=1}^n (y_i - \bar{y})^2, \\ S_{xy} &= \sum_{i=1}^n (x_i - \bar{x})(y_i - \bar{y}). \end{aligned}$$

In order to compute the covariance  $C_l = \begin{bmatrix} \sigma_\rho^2 & \sigma_{\rho\alpha} \\ \sigma_{\alpha\rho} & \sigma_\alpha^2 \end{bmatrix}$  of the parameters  $[\rho^*, \alpha^*]'$ , let  $A_i$  be the Jacobian matrix of  $f(\cdot)$  w.r.t.  $[x_i, y_i]'$ :

$$A_i = \begin{bmatrix} \frac{\partial f_1}{\partial x_i} & \frac{\partial f_1}{\partial y_i} \\ \frac{\partial f_2}{\partial x_i} & \frac{\partial f_2}{\partial y_i} \end{bmatrix}.$$

Denoting by  $C_{p_i}$  the covariance matrix of a point  $p_i = [x_i, y_i]'$ , under the hypothesis that  $p_i, p_j$  are uncorrelated if  $i \neq j$ ,  $C_l$  is given by  $C_l = \sum_{i=1}^n A_i C_{p_i} A_i'$ . By exploiting the following relationships:

$$\begin{aligned} \frac{\partial S_{xy}}{\partial x_i} &= y_i - \bar{y}, & \frac{\partial S_{xy}}{\partial y_i} &= x_i - \bar{x}, \\ \frac{\partial S_{x^2}}{\partial x_i} &= 2(x_i - \bar{x}), & \frac{\partial S_{y^2}}{\partial y_i} &= 2(y_i - \bar{y}), \\ \frac{\partial S_{y^2}}{\partial x_i} &= 0, & \frac{\partial S_{x^2}}{\partial y_i} &= 0, \end{aligned}$$

it can be shown that the Jacobian matrix has the expression:

$$A_i = \begin{bmatrix} A_i(1, 1) & A_i(1, 2) \\ A_i(2, 1) & A_i(2, 2) \end{bmatrix},$$

where:

$$\begin{aligned} A_i(1, 1) &= \frac{\cos(\alpha^*)}{n} - \bar{x} \sin(\alpha^*) A_i(2, 1) + \\ &\quad + \bar{y} \cos(\alpha^*) A_i(2, 1), \\ A_i(1, 2) &= \frac{\sin(\alpha^*)}{n} - \bar{x} \sin(\alpha^*) A_i(2, 2) + \\ &\quad + \bar{y} \cos(\alpha^*) A_i(2, 2), \\ A_i(2, 1) &= \frac{(\bar{y} - y_i)(S_{y^2} - S_{x^2}) + 2S_{xy}(\bar{x} - x_i)}{(S_{y^2} - S_{x^2})^2 + 4S_{xy}^2}, \\ A_i(2, 2) &= \frac{(\bar{x} - x_i)(S_{y^2} - S_{x^2}) - 2S_{xy}(\bar{y} - y_i)}{(S_{y^2} - S_{x^2})^2 + 4S_{xy}^2}. \end{aligned}$$

Finally, if the polar coordinates  $[d_i, \phi_i]$  of the points  $p_i$  are available, together with the corresponding covariance matrix  $C_{m_i} = \begin{bmatrix} \sigma_{d_i}^2 & \sigma_{d_i\phi_i} \\ \sigma_{\phi_i d_i} & \sigma_{\phi_i}^2 \end{bmatrix}$ , the covariance matrix  $C_{p_i}$  must be expressed in terms of  $C_{m_i}$ . Denote by  $g(d_i, \phi_i)$  the coordinate transformation:

$$\begin{bmatrix} x_i \\ y_i \end{bmatrix} = \begin{bmatrix} d_i \cos(\phi_i) \\ d_i \sin(\phi_i) \end{bmatrix} \triangleq \begin{bmatrix} g_1(d_i, \phi_i) \\ g_2(d_i, \phi_i) \end{bmatrix}. \quad (12)$$

Then, the optimal line parameters are given by  $[\rho^*, \alpha^*]'$  =  $s(d_1, \phi_1, \dots, d_n, \phi_n)$ , obtained by substituting equation (12) into (11). Moreover, the covariance matrix  $C_l$  of  $[\rho^*, \alpha^*]'$  can be computed as  $C_l = \sum_{i=1}^n J_i C_{m_i} J_i'$ , where  $J_i = A_i B_i$  and

$$B_i = \begin{bmatrix} \frac{\partial g_1}{\partial d_i} & \frac{\partial g_1}{\partial \phi_i} \\ \frac{\partial g_2}{\partial d_i} & \frac{\partial g_2}{\partial \phi_i} \end{bmatrix} = \begin{bmatrix} \cos(\phi_i) & -d_i \sin(\phi_i) \\ \sin(\phi_i) & d_i \cos(\phi_i) \end{bmatrix}.$$

## REFERENCES

- [1] S. Thrun, "Robotic mapping: a survey," in *Exploring Artificial Intelligence in the New Millenium*, G. Lakemeyer and B. Nebel, Eds. Morgan Kaufmann, 2002.
- [2] J. J. Leonard and H. F. Durrant-Whyte, "Mobile robot localization by tracking geometric beacons," *IEEE Transactions on Robotics and Automation*, vol. 7, no. 3, pp. 376–382, 1991.
- [3] M. Dissanayake, P. Newman, S. Clark, H. Durrant-Whyte, and M. Csorba, "A solution to the simultaneous localization and map building (SLAM) problem," *IEEE Transactions Robotics and Automation*, vol. 17, no. 3, pp. 229–241, 2001.
- [4] A. Garulli and A. Vicino, "Set membership localization of mobile robots via angle measurements," *IEEE Transactions on Robotics and Automation*, vol. 17, no. 4, pp. 450–463, August 2001.
- [5] K. Briechle and U. D. Hanebeck, "Localization of mobile robot using relative bearing measurements," *IEEE Transactions on Robotics and Automation*, vol. 20, no. 1, pp. 36–44, February 2004.
- [6] M. Di Marco, A. Garulli, A. Giannitrapani, and A. Vicino, "A set theoretic approach to dynamic robot localization and mapping," *Autonomous Robots*, vol. 16, pp. 23–47, January 2004.
- [7] I. J. Cox, "Blanche - an experiment in guidance and navigation of an autonomous mobile robot," *IEEE Transactions on Robotics and Automation*, vol. 7, no. 3, pp. 193–204, 1991.
- [8] F. Lu and E. Miliotis, "Robot pose estimation in unknown environments by matching 2D range scans," *Journal of Intelligent and Robotic Systems*, vol. 18, pp. 249–275, 1997.
- [9] J. Vandorpe, H. Van Brussels, and H. Xu, "Exact dynamic map building for a mobile robot using geometrical primitives produced by a 2d range finder," in *Proceedings of the 1996 IEEE International Conference on Robotics and Automation*, Minneapolis, April 1996, pp. 901–908.
- [10] A. T. Pfister, S. I. Roumeliotis, and J. W. Burdick, "Weighted line fitting algorithms for mobile robot map building and efficient data representation," in *Proceedings of the 2003 IEEE International Conference on Robotics and Automation*, Taiwan, September 2003, pp. 1304–1311.
- [11] O. Wulf, K. O. Arras, H. I. Christensen, and B. Wagner, "2D mapping of cluttered indoor environments by means of 3D perception," in *Proceedings of the 2004 IEEE International Conference on Robotics and Automation*, New Orleans, LA, April 2004, pp. 4204–4209.
- [12] J. J. Leonard, P. M. Newman, R. J. Rikoski, J. Neira, and J. D. Tardós, "Towards robust data association and feature modeling for concurrent mapping and localization," in *Proceedings of the Tenth International Symposium on Robotics Research Lorne*, Victoria, Australia, November 2001.
- [13] S. J. Julier and J. K. Uhlmann, "A counter example to the theory of simultaneous localization and map building," in *Proceedings of the 2001 IEEE International Conference on Robotics and Automation*, May 2001, pp. 4238–4243.